Investigating Side Chain Mediated Electroluminescence from Carbazole-Modified Polyfluorene

Jin-Long Liao,[†] Xiwen Chen,[†,‡] Ching-Yang Liu,[†] Show-An Chen,*[,†] Chiu-Huen Su,[§] and An-Chung Su[†,§]

Department of Chemical Engineering, National Tsing-Hua University, Hsinchu, 30013 Taiwan, Republic of China, and Institute of Materials Science and Engineering, National Sun Yat-sen University, Kaohsiung 804, Taiwan, Republic of China

Received: November 28, 2006; In Final Form: June 28, 2007

In molecular design of electroluminescent (EL) conjugated polymers, introducing a charge transport moiety on a side chain is found to be a promising method for balancing electron and hole fluxes in EL devices without changing the emitting color if there is no interaction between moiety and main chain. In the case of grafting a carbazole (Cz) moiety (hole transporting) on blue emitting polyfluorene, a green emission appears with intensity comparable to the blue emission, which was attributed to a possible interaction between main chain and Cz as previously reported by us. Here, a detailed study of its EL mechanism was carried out by means of time-resolved EL with the assistance of molecular simulation and thermally stimulated current measurements; exploration of how main chain segments interact with the transport moiety was performed. We found the Cz groups in Cz100PF play multiple roles: they act as (1) hole transporter to improve hole injection, (2) hole trapping site for efficient electron-hole recombination to yield blue-emitting excitons, and (3) source of green emission from electroplex formed via electric field-mediated interaction of the Cz/Cz radical cation with an electron in the nearby PF backbone. In combination, these observations suggest that integrated consideration for both intramolecular and intermolecular interactions provides a new route of molecular design of efficient EL polymers.

Introduction

Charge injection and charge mobility are two crucial factors in designing electroluminescent (EL) polymers for polymer light emitting diodes (PLED). The most studied EL polymers are poly(phenylene vinylene)s (PPVs) and polyfluorenes (PFs),[1] which have been found to be hole transport-dominated materials because their hole mobilities are 1−3 orders higher than their electron mobilities.[2] Extensive efforts have been made for developing new emissive semiconducting polymers with improved electron transport characteristics via the introduction of electron-deficient moieties inserted in the backbone through straightforward copolymerization[3] or attached directly onto (and in conjugation with) the backbone;[4] in both cases, the emissive wavelength is often altered. A more attractive alternative is to attach the electron deficient group at the end of a long flexible spacer linked to the backbone[5] as reported by us[5a,b,e] and others[5c,d] for designing EL polymers by modifying the hole dominating soluble poly(*p*-phenylene vinylene) through introducing a proper amount of the typical electron deficient moiety, the oxadiazole (OXD) group, on ends of its long flexible side chains. Such modification in addition leads to a more amorphous chain arrangement such that the OXD moieties are dispersed uniformly in the main chain matrix.[5b] The device prepared has a low turn-on voltage and high EL efficiency. We also reported[5e] that the hole-dominating soluble PPV was modified through introducing the highly electron-deficient moiety, the triazole (TAZ) group, on ends of its long flexible side chains, allowing a conversion from hole-dominated transport to electron-dominated transport. The device prepared has a high EL efficiency due to a balance of charge carrier mobilities and densities. For polyfluorenes, similar modifications by introducing OXD[6a] and additional hole-transporting triphenylamine[6b] as side chains at the C-9 position also have been attempted. This approach is adopted based on the consideration that no interaction occurs between the transport moiety and the conjugated main chain and thus can be termed as a single chain consideration.

Interactions between the charge transport moiety and the conjugated main chain, however, can be expected to occur in two ways: (a) by directly attaching to repeat units or polymer chain ends with a conjugation interaction in their π-systems at the ground state[7] and (b) through molecular stacking such that the interaction occurs at the excited state under electric fields[8a] (electroplex or electromer formation).[8b,c,d] The electroplex (M^+N^-) is an electronically excited emitting species, which forms only under an electric field by cross-recombination of electrons in the acceptor (N) and the holes in the donor (M) molecules (or segments).[8b] The electroplex is an analogue of the photoexcited emitting species, exciplex (M*N), in which the donor molecule is at the excited state M* and the acceptor molecule is at the ground state N. In both cases, if M and N are of the same kind of molecule (or segments), the complex pairs are termed electromer[8d] and excimer,[8e] respectively. Note that the essential difference in structure between the electroplex and the exciplex is that the former involves a cross-recombination of the radical cation (M^+) and radical anion (N^-), while the latter involves a charge transfer interaction between M* and N.

* Corresponding author. E-mail: sachen@che.nthu.edu.tw.
† National Tsing-Hua University.
‡ Present address: Department of Chemistry, Simon Fraser University, 8888 University Dr., Burnaby, BC, V5A 1S6, Canada.
§ National Sun Yat-sen University.

10.1021/jp067878i CCC: $37.00
Published on Web 08/15/2007

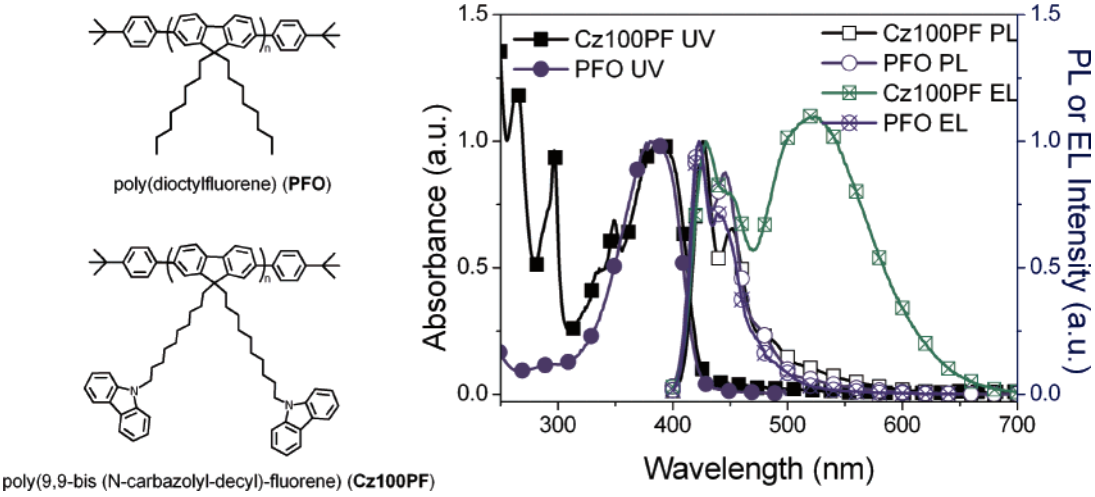

Figure 1. Chemical structures and optical spectra (UV, PL, and EL) of PFO and Cz100PF.

For case a, the interaction at the ground state, we[7] capped both ends of the poly(dioctyl fluorene) (PFO; its chemical structure is shown in Figure 1) chain with electron-deficient moieties (OXD and TAZ), which can induce a minor amount of long conjugating length species (regarded as the β-phase) to allow for incomplete energy transfer from the amorphous matrix to the β-phase. Consequently, the resulting EL spectrum consists of two blue emitting peaks from the amorphous and β-phases together with a weaker longer wavelength tail and provides stable, promoted device efficiency and, especially for TAZ, pure blue emission during cyclic operations with the Commission Internationale de l'Eclairage (C.I.E.) coordinates ($x = 0.165$, $y = 0.076$). For the high triplet polymer, poly(3,6−9-octylcarbazole) (P(3,6-Cz)),[9] we have modified the repeat unit via the 9 position of Cz by attaching a di-*t*-butyl-carbazole unit spaced by a biphenyl to yield P(*t*-Bu-CBP). Such modification leads to a lowering of the HOMO level (as well as the LUMO level) with respect to P(3,6-Cz) by about 0.3 eV (0.2 eV) due to the inductive acceptor effect provided by the side group (biphenylcarbazole) and causes a balance of charge fluxes by promoting electron injection and reducing hole injection relative to P(3,6-Cz). Upon doping with green and red emission Ir complexes, devices with high luminous and external quantum efficiencies for green emission ($\eta_{Lmax} = 23.7$ cd A^{-1}, $Q_{ext} = 6.57\%$) and for red emission ($\eta_{Lmax} = 5.1$ cd/A, $Q_{ext} = 4.23\%$) are generated, respectively. For both devices, the efficiencies are higher than those of the corresponding devices with P(3,6-Cz) as the host by a factor of 4, even though the latter has an E_T (2.6 eV) value slightly higher than P(*t*-Bu-CBP).

For case b, with the molecular stacking of the transport moieties along with an interaction with the main chain under electric field, we[8a] have incorporated Cz groups on the end of the alkyl side chains of poly(dialkylfluorene) for a promotion of hole injection. However, additional green emission appears, which was attributed to a possible cross-recombination of electrons in a main chain segment and a hole in a nearby side chain Cz, that is, the formation of the electroplex, which will be revealed in more detail later. Such green emission did not result from a fluorenone defect[10] as was studied in great detail by us.[11a] Upon doping with a phosphor dopant of a red emission cyclometalated iridium complex, the device prepared emitted red−green−blue simultaneously or red alone depending on the dopant concentration. This observation indicates that the transport moiety plays multiple roles and that its interaction with the main chain provides a new route for the molecular design of EL polymers, which deserves detailed study of the interaction as well as the emission mechanism.

Here, a detailed study of the emission mechanism of the devices based on a carbazole-capped dialkyl side chain-modified polyflorene (Cz100PF; see Figure 1 for its chemical structure) was carried out. By means of time-resolved (TR) EL with the assistance of molecular simulation (MS) as well as thermally stimulated current (TSC) and time-of-flight (TOF) measurements, the exploration as to how main chain segments interact with the transport moieties was carried out. We found that the Cz moiety in fact plays multiple roles in electroluminescence that the blue emission originates from the PF backbone, and that the green emission originates from the electroplex formed between the stacked Cz/Cz dimer and the nearby main chain segment under the applied electric field. In combination, these observations suggest that integrated consideration for both intramolecular and intermolecular interactions provides a new route of molecular design of efficient EL polymers.

Experimental Procedures

Materials, Device Fabrication, and General Instrumentation. PFO and Cz100PF were synthesized by the Yamamoto reaction.[8a] Indium−tin oxide (ITO) glass plates were treated with oxygen plasma before spin-coating of a thin (ca. 30 nm) hole injection layer of poly(styrene sulfonic acid) doped poly(ethylenedioxythiophene) (PEDOT/PSS, designated as PEDOT for simplicity; Baytron P CH 8000 from Bayer, ca. 10^{-5} S cm^{-1} conductivity). On top of this, a thin layer (ca. 100 nm) of emitting polymer was spin-cast from its solution (10 mg mL^{-1}) in chloroform or THF. Finally, a thin layer of calcium (about 5 nm) covered with a layer of aluminum as the cathode for the bipolar device was deposited in a vacuum thermal evaporator through a shadow mask at a pressure of less than 2×10^{-6} Torr. The active area of the diode was about 10 mm^2. A surface profiler (Tencor P-10) was used for determining the polymer film thickness. UV−vis spectra were recorded by use of a PerkinElmer Lambda-19 spectrometer. Photoluminescence (PL) and EL spectra were obtained using a fluorescence spectrometer (Jobin-Yvon, FluoroMax-3).

TSC Measurements.[12] The existence of a trap and its energy level, concentration, and polarity in organic materials have been successfully investigated by using the thermally stimulated current (TSC) technique. In the fabrication of a device for TSC measurement, a polymer film (ca. 0.8 μm in thickness) was spin-

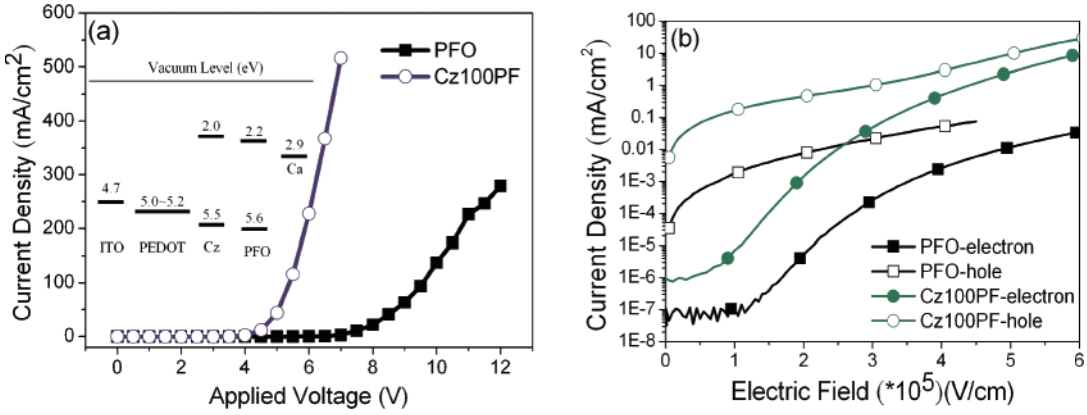

Figure 2. (a) Current density characteristics for bipolar devices (ITO/PEDOT/polymer/Ca/Al) with PFO and Cz100PF as the active polymer layer. (b) Hole and electron current density characteristics for hole-dominated devices (ITO/PEDOT/polymer/Au) and electron-dominated devices (ITO/Ca/polymer/Ca/Al) with PFO and Cz100PF as the active polymer layer. Inset is the band diagram of the materials used and the Cz group.

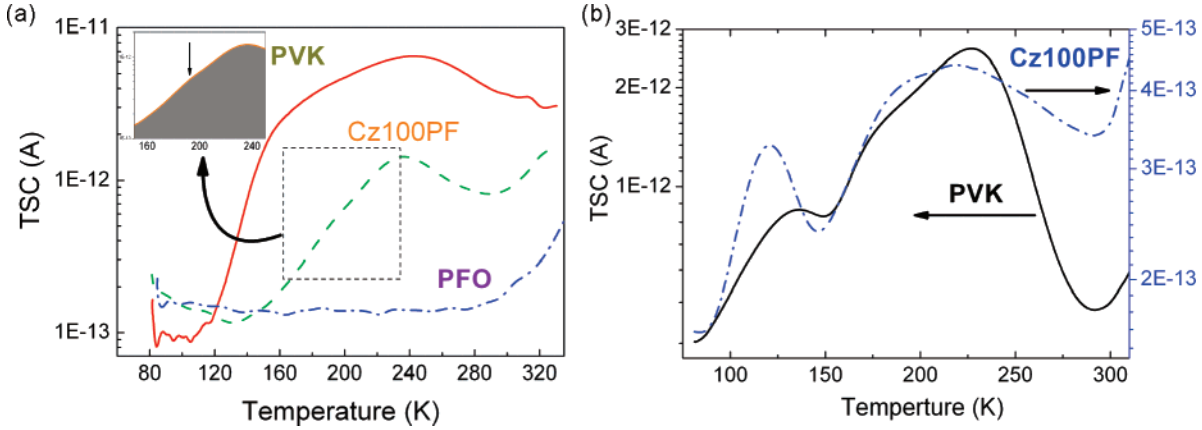

Figure 3. (a) PE TSC spectra of PFO, Cz100PF, and PVK, obtained from ITO/polymer/Al devices after white light excitation at 80 K for 10 min (b) FI TSC spectra of Cz100PF and PVK, obtained from ITO/polymer/Au devices after applying a field of 5×10^5 V/cm for 10 min. Temperature and thermally stimulated current were recorded every 3 s (i.e., sampling frequency 2 points/K).

coated from its chloroform solution (10 mg mL^{-1}) on an ITO glass plate, then was covered by a layer of aluminum (ca. 100 nm thickness) as the cathode for the photoexcited (PE) TSC measurements or a layer of gold (ca. 30 nm thickness) for field-induced (FI) TSC measurements. In the TSC measurements, the device was mounted in a cryostat (Model 475, Jenis) under vacuum (10^{-5} Torr), and its temperature could be controlled by heating at a specific constant rate (10 K/min) from 80 to 330 K. The thermally stimulated current was measured by connection to a Keithley power supply (Model 238). For PE TSC measurements, the traps were filled at 80 K by irradiating with a 70 W xenon lamp for 10 min. For FI TSC measurements, the device was applied at an electrical field of 5×10^5 V cm^{-1} for 10 min at 80 K. After the trap filling, waiting periods of 10 and 30 min for PE TSC and for FI− TSC, respectively, were allocated so that the discharging current was reduced to a negligible level. The device was then used at a fixed heating rate of 10 K min^{-1} with zero bias while recording the temperature and the thermally stimulated current versus temperature every 3 s (i.e., sampling frequency 2 points/K).

TOF Measurements.[8a] Devices for TOF measurement were prepared by spin-casting polymer films (1−3 μm thickness) from toluene solutions on pretreated ITO coated glass substrates in a glove box with argon. Aluminum as the charge collection electrode was then deposited by thermal evaporation (at 10^{-6} Torr) through a shadow mask. All devices were mounted in a cryostat, and measurements were taken at room temperature under a vacuum of less than 10^{-6} Torr. The photocurrent was generated by a nitrogen-laser-pumped dye laser at 390 nm with a pulse width of 500 ps through the transparent ITO electrode. The transient current was measured across the load resistor using a 500 MHz digital storage oscilloscope. The drift mobility of the carriers (holes in this case) under a positive electric field to the collecting electrode resulted in a time-dependent current. The hole mobility (μ) is related to the transit time by the relation $\mu = d/t_T E$, where d is the film thickness and E the external electric field.

Time-Resolved EL Spectroscopy (TREL). TREL spectra were obtained using a pulse generator (AV-1012-B, AVTECH) to apply a narrow voltage pulse (1 MHz, pulse width 200 ns at 6 V for Cz100PF) to the device in a cryostat under vacuum (5×10^{-6} Torr) at room temperature. A series of luminescence decay curves at specific wavelengths (a decay curve for every 5 nm from 365 to 650 nm was taken, and every decay curve was measured with the same time period of 5 min) were measured using a 4096-channel time-correlated single photon counting (TCSPC) system with a microchannel plate photomultiplier tube (Hamamatsu Photonics R3809U-50) and a spectrometer (Edinburgh, Lifespec-ps with TCC900 data acquisition card). The TREL spectra were obtained by using the function TRES in the fluorescence spectrometer software F900. The experimental setup and typical trigger−pulse−EL responses are shown in Figure 6.

Molecular Simulation. Molecular simulation studies were performed on a SGI Origin 3800 workstation equipped with the Cerius 2 package (version 4.9, Accelrys). The universal force field (UFF, version 1.02) was selected. A cutoff distance of 1.0 nm for van der Waals potentials was consistently adopted

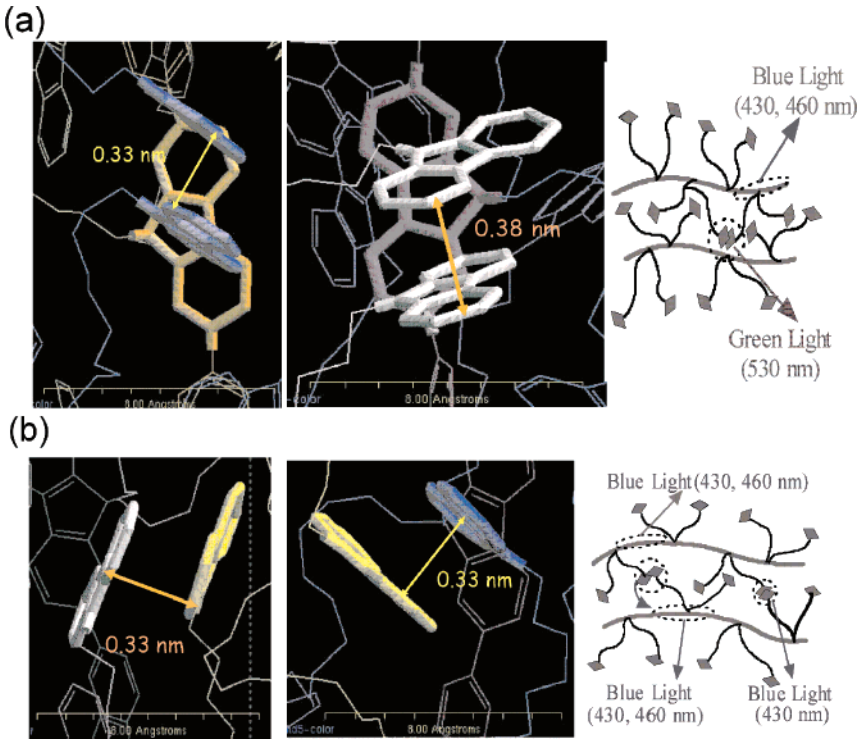

Figure 4. Molecular arrangements (as obtained from molecular dynamics simulations) and schematic illustration of Cz−dimer configurations that may serve as sites for (a) electroplex and (b) excimer formation. Note that the orange or blue vertical segment in panel a corresponds to a PF backbone repeat unit.

throughout the molecular simulation process. In the case of Cz100PF, five chains (each with 10 repeat units) were arranged in a low-density tetragonal unit cell, with the space group assigned as *P*1 and adopting periodic boundary conditions. The unit cell dimensions (first *a*- and *b*-axes and then *c*-axis for final minor adjustment) were stepwise shortened (2−3% in the earlier stage but 0.3−0.35% in later steps) and energy minimized. The procedure was repeated until the system energy reached a minimum, which corresponded to ca. 0.98 g/mL density. A molecular dynamics (MD) simulation was then performed by setting the temperature as 298 K until reaching a thermal equilibrium. Molecular packing in the unit cell was then examined visually on the screen.

Results and Discussion

Optical Spectroscopy. Figure 1 shows the UV, PL, and EL spectra of PFO and Cz100PF. The absorption and PL spectra of these two polymers are essentially the same in the ranges of 300−450 and 400−600 nm, respectively, except for the two additional absorption peaks for Cz100PF at 300 and 270 nm originating from the carbazole and benzene ring. However, their EL spectra from the devices, ITO/CFx/polymer/CsF/Ca/Al, are dramatically different; the PFO device emits blue light (C.I.E coordinates: 0.17, 0.15) with two characteristic peaks at 420 and 450 nm, while the Cz100PF device emits sky blue light (C.I.E coordinates: 0.23, 0.30) with two characteristic peaks at 420 and 460 nm as for PFO and an additional strong broad peak at 525 nm and has a turn-on voltage of 3.3 V, maximum efficiency of 4.98 cd A^{-1}, and maximum brightness of 27 000 cd m^{-2}. The broad emission around 525 nm does not exist in the corresponding PL spectrum. Since this green emission turns on at the beginning of the device operation, it should not come from a degradation of the device.[1d] This green emission cannot be attributed to the excimer emission of stacked Cz/Cz groups (Cz/Cz dimer), as the excimer emission peaks are at 370 nm (partial overlap) or 420 nm (face-to-face overlap) in PVK.[13] Neither can it be assigned to electromer emission[14] of Cz/Cz

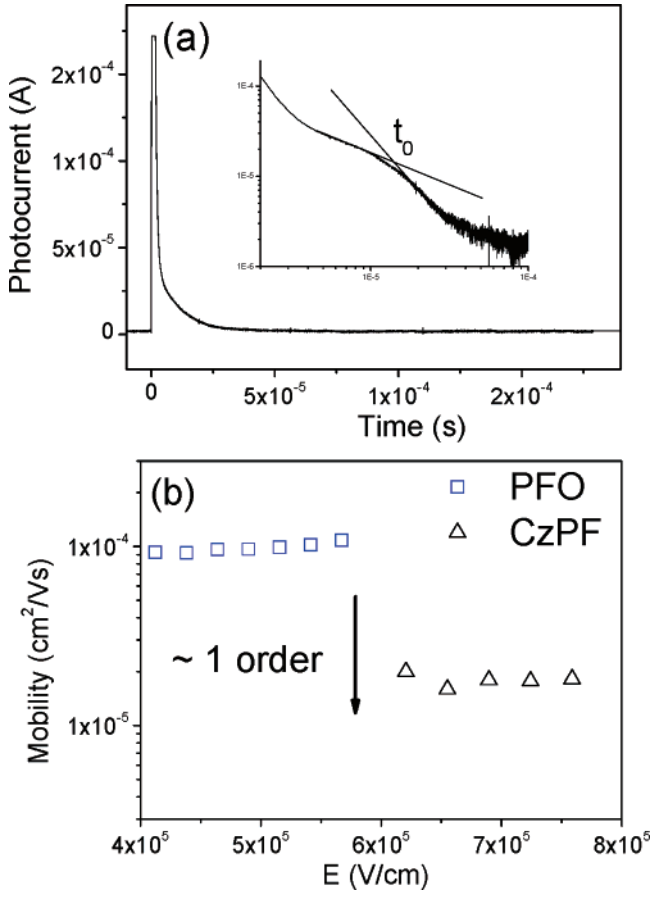

Figure 5. Results of time-of-flight measurements for PFO and Cz100PF: (a) typical current profile vs time of Cz100PF and (b) mobility vs applied electric field.

dimers, which emit at 610 nm. Moreover, as both of our polymers are end-capped,[11] the possibility of the end-group effect due to the use of an uncapped polymer can be safely excluded. Here, we propose that this broad green emission originates from the electroplex[8] formed by the Cz/Cz dimer interacting with the PF backbone under an electrical field as to be revealed in detail later.

Bipolar and Single Carrier Devices. Figure 2a,b shows the current density characteristic of the bipolar and single carrier (electron- and hole-dominated) devices with PFO and Cz100PF as the active layers, respectively. The current density of Cz100PF is 170 times higher than that of PFO under the same applied electric field (7×10^5 V/cm) (shown in Figure 2a). In terms of the band diagram[8a] of the PFO and Cz moiety (inset in Figure 2a), the hole-injection barrier between the PEDOT and the Cz moiety (0.3 to ~0.5 eV) is lower than that between PEDOT and PFO (0.4 to ~0.6 eV). It is very clear that introducing the Cz moiety into the side chain of PF reduces the hole-injection barrier at the PEDOT−polymer interface and improves the charge transport in Cz100PF. Moreover, the charge transport properties of Cz100PF and PFO provided by the single-carrier (electron- and hole-dominated) devices are analyzed next. For PFO, the current density of the holes is higher than that of electrons by 2 orders of magnitude at 3×10^5 V/cm, while Cz100PF shows higher and more balanced electron and hole fluxes than PFO. The electron-injection barrier height of Cz (0.9 eV, relative to Ca) is higher than that of PFO (0.7 eV), implying that the electron injection becomes more difficult for Cz100PF. Since the factors that influence current density are the carrier number and carrier mobility and the electron current density of Cz100PF is also higher than that of PFO, Cz contributes to an improvement in electron mobility. It is obvious that the higher and more balanced electron and hole fluxes of Cz100PF originate from the incorporation of the Cz moiety. These results also indicate that Cz is ambipolar in nature and can promote both hole and electron fluxes and reduce the hole-injection barrier.

Charge Trapping in Cz/Cz Pair and Electroplex Formation in Cz100PF: Thermally Stimulated Current and Time-of-Flight Measurements. To investigate if any possible stacking of Cz groups in Cz100PF occurs and how the stacking affects its charge transport characteristics, we compare Cz100PF with poly(vinyl cabazole) (PVK) on their charge trapping characteristics. Previous studies indicated the presence of two kinds of excimers in PVK, the partially overlapped excimer and the face-to-face excimer, both acting as hole-trapping sites.[15] Figure 3a shows photoexcited thermally stimulated current (PE TSC)[12a,c] profiles of unmodified PF (PFO), Cz100PF, and PVK. Cz100PF exists as a peak at 235 K and a shoulder at 195 K; for PVK, a similar spectrum is observed, having a peak at 240 K and a shoulder at 180 K. However, no trapped current was observed for PFO, for which the upturn current starting at 275 K was due to the dark current. It is hence obvious that the trapped current of Cz100PF originates from Cz moieties, not from the PF backbone. It is impossible to use PE TSC to identify the polarity of the trap current since photoexcitation can generate both hole and electron currents. To identify the trap polarity in Cz100PF and PVK, hole-dominated devices were used for FI thermally stimulated current (FI− TSC)[12b,c] measurements, allowing that only holes can be injected into the polymer layer. As can be seen, similar profiles are shown in Figure 3b. For Cz100PF and PVK, two peaks are clearly observed for each case; the one at low temperatures (120 and 130 K, respectively) does not appear in the corresponding PE TSC spectra of the

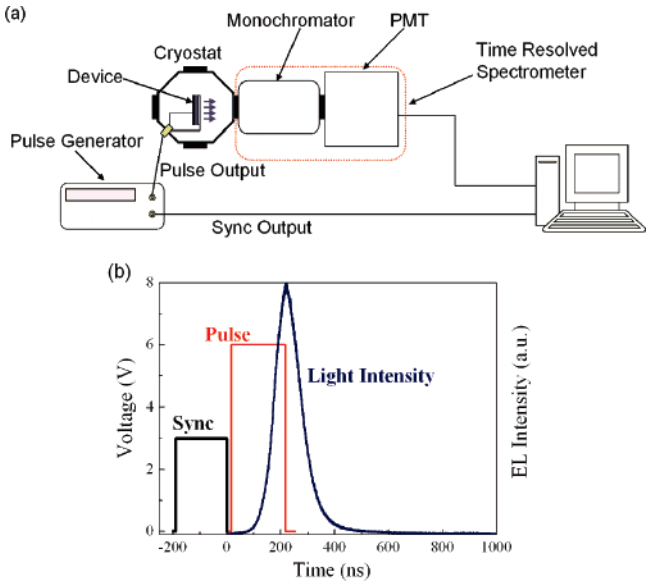

Figure 6. (a) Experimental setup for TREL. (b) Trigger−pulse−EL sequence adopted for ITO/PEDOT/Cz100PF/Ca/Al devices.

bipolar devices of Cz100PF and PVK, indicating that it is a thermally stimulated depolarization current,[12d] as also is evidenced by the appearance of a symmetric peak upon reversed bias. The other at the higher temperatures of 220 K (with a shoulder at 185 K) and 230 K (with a shoulder at 185 K), respectively, have PE TSC counterparts and hence can be attributed to the hole-trapped current. These observations not only confirm that the trapped currents in Cz100PF, as in PVK, are due to hole traps, but also indicate the formation of hole-trapping excimers in Cz100PF upon photoexcitation. Results of MD simulation (Figure 4) are in support of the presence of closely arranged Cz groups in the form of nearly face-to-face (Figure 4a) or partially overlapped pairs (Figure 4b), the Cz/Cz pair in contact with the PF backbone (Figure 4a, left), as well as random and disoriented contacts between Cz groups. In these Cz/Cz pairs, face-to-face distances lie in the range of 0.33−0.38 nm, similar to those reported for PVK (0.34−0.38 nm).[16] The fractions of face-to-face stacking, partially overlapped stacking, and random Cz moieties are 4, 20, and 76%, respectively. This molecular simulation result can explain why the hole current density of Cz100PF is still larger than that of PFO even though hole traps (Cz/Cz dimer) exist in the former. The reason is that, in Cz100PF, however, the fraction of random Cz moieties (76%) is much higher than Cz groups appearing as Cz/Cz dimers (24%). These random Cz moieties act in two roles in Cz100PF: (a) the reduction of the hole-injection barrier and (b) the promotion of hole transport.

Further confirmation of the occurrence of charge trapping in Cz/Cz pairs is made by the measurement of hole mobility under various electric fields for PFO and Cz100PF at room temperature using the time-of-flight method as shown in Figure 5. As can be seen, the current profiles for Cz100PF are rather dispersive (Figure 5a), while those for PFO are nondispersive. The hole mobility of PFO (about 1×10^{-4} cm^2/V s) is higher than that of Cz100PF (about 1×10^{-5} cm^2/V s) by 1 order of magnitude, confirming that charge trapping occurs in Cz100PF. The hole mobilities of both polymers are weakly field dependent.

EL Spectral Dynamics: TREL. To explore the origin of the broadband green emission in Cz100PF, which appears in EL but not in PL spectra (Figure 1), we have performed TREL measurements (the experimental setup and condition are shown in Figure 6). Normalized EL spectral dynamics (in 10 ns

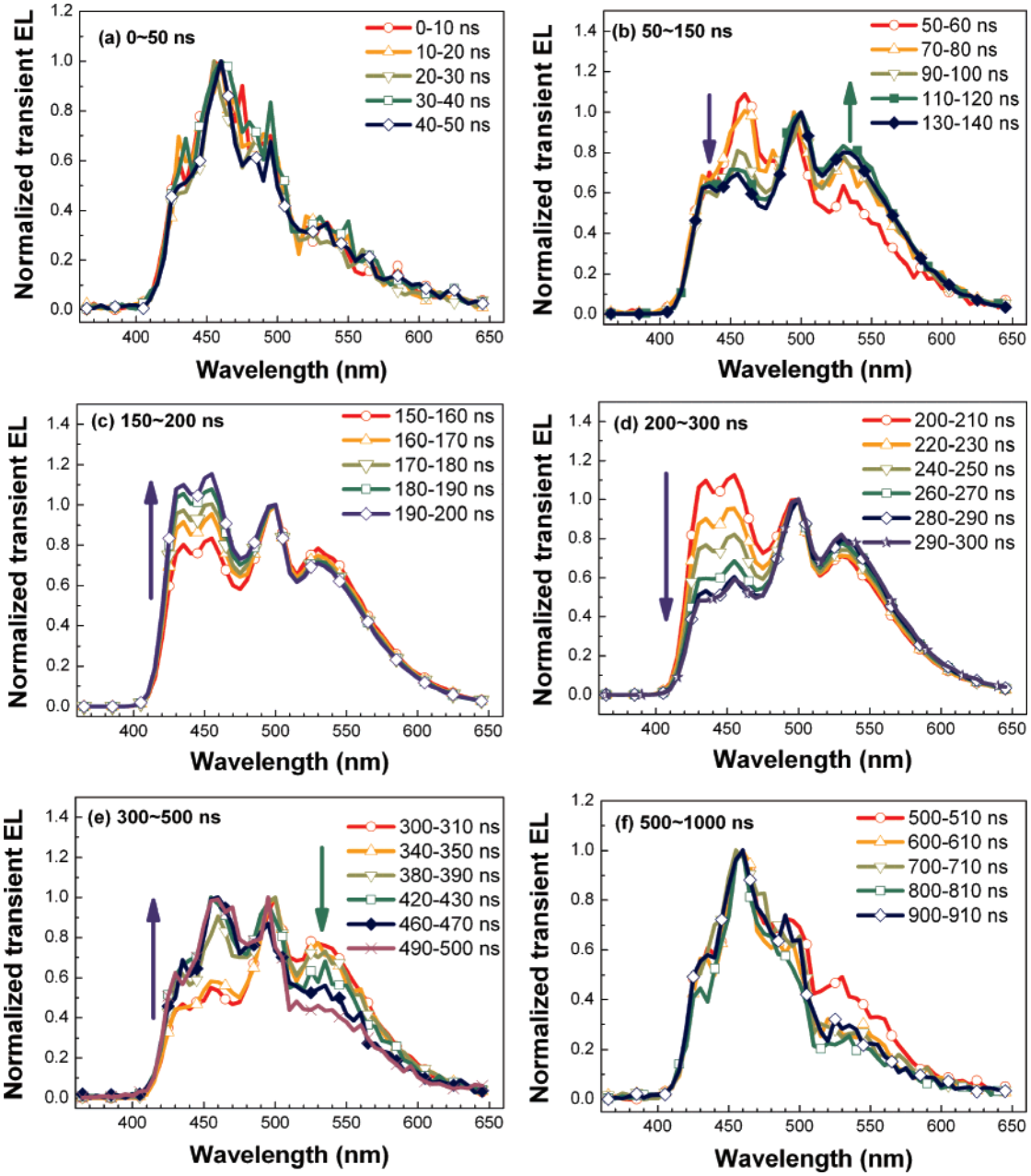

Figure 7. Normalized EL spectral dynamics of Cz100PF in different time periods after triggering a pulsed (200 ns in width) electric field excitation: (a) 0−50 ns, (b) 50−150 ns, (c) 150−200 ns, (d) 200−300 ns (first period beyond electric field excitation), (e) 300−500 ns, and (f) 500−1000 ns. Spectra in panels a and f are normalized at 460 nm; spectra in panels b−e are normalized at 490 nm.

intervals throughout the 1 μs cycle period) of Cz100PF is shown in Figure 7, for which the first 200 ns period corresponds to the electro-excitation pulse. In the early stage of electro-excitation (phase A, t = 0−50 ns, Figure 7a), TREL spectra similar to the steady-state EL spectrum of PFO are obtained, indicating the dominant contribution from singlet excitons formed along the PF backbones. In the next period of t = 50−150 ns (phase B, Figure 7b), TREL spectra exhibit clear variations: the intensity of green emission (530 nm) increases, whereas that of blue emission (430 and 460 nm) decreases with time. In the last period of charge injection (phase C, t = 150 to ~200 ns, Figure 7c), the intensity of blue emission at 430 and 460 nm rises, which decreases again after the termination of charge injection (phase D, t = 200−300 ns, Figure 7d). In the followed period (phase E, t = 300−500 ns, Figure 7e), the relative intensity of the green emission decreases continuously, leaving only blue emission in the final period (phase F, t = 500−1000 ns, Figure 7f).

On the basis of current understanding of the hole-trapping characteristics of Cz/Cz dimers, we propose spectral dynamics as follows. In phase A, electrons and holes begin to be injected into the emitting layer and transport along the PF backbones. They may combine to result in singlet excitons, which then relax and emit blue light. In the meantime, some holes can be trapped on Cz/Cz dimers to yield Cz/Cz dimer radical cations by stabilization through π-system interactions.[14c] With continuing charge injection in phase B, cross-combination of the Cz/Cz radical cations with electrons located at nearby PF backbones results in the lower energy green emission. Because this broadband emission is observed only in the EL but not in the PL spectra, the emitting species should be categorized as electroplex,[8] for which electric FI orientation/stabilization is expected to play a role (phases A and B are sketched in Figure 4a). Such electronically excited species yielded by cross-recombination can be expressed as [(Cz/Cz dimer)$^+$(main chain fluorene segments)$^-$]. Although the electroplex contains three

components, it is actually a two-component complex since only the Cz/Cz dimer can act as a hole trap and become a stable radical cation after catching a hole. This radical cation can then recombine with a nearby radical anion main chain fluorene segment with a proper orientation. The increase in relative intensity of the blue emission in phase C is most likely due to relaxation of the Cz/Cz excimers located distantly from the PF backbones, as the emission at 430 nm (characteristic of the sandwich Cz/Cz excimer) is particularly strong as compared to the spectra in Figure 7a. (It is conceivable that some of the excimers may transfer energy to the PF backbones to emit blue light.) In phase D, the decrease in relative intensity of blue emission is attributed to a consumption of holes trapped on Cz/Cz excimers distant from the PF backbone. In phase E, the decrease in intensity of the green emission is due to an exhaustion of holes trapped on Cz/Cz excimers located close to the PF backbones, leading to a complete depletion of holes trapped on the Cz/Cz excimers in the final stage, phase F (phases D−F are sketched in Figure 4b).

Conclusion

In summary, we find that the Cz groups in Cz100PF play multiple roles: they act (a) as a hole transporter at the polymer−PEDOT interface to provide an ease of hole injection, (b) as a hole trapping site (in the form of Cz/Cz dimers) for efficient electron−hole recombination to yield blue emitting excitons, and (c) as a source of green emission from an electroplex formed via electric field-mediated interaction of the Cz/Cz radical cation with electrons in the nearby PF backbone. The present observations point to the need of integrated considerations of both intramolecular and intermolecular interactions in designing EL polymers for color tuning with improved brightness and efficiency.

Acknowledgment. We thank the Ministry of Education (Project 91E-FA04-2-4A) and the National Science Council (Projects 95E-2752-E007-005 and 008-PAE) for financial support and the National Center for High-Performance Computing for computer time and facilities.

References and Notes

(1) (a) Friend, R. H.; Gymer, R. W.; Holmes, A. B.; Burroughes, J. H.; Marks, R. N.; Taliani, C.; Bradley, D. D. C.; Dos Santos, D. A.; Brédas, J. L.; Lögdlund, M.; Salaneck, W. R. *Nature* **1999**, *397*, 121. (b) Ho, P. K. H.; Burroughes, J. H.; Becker, H.; Li, S. F. Y.; Brown, T. M.; Cacialli, F.; Friend, R. H. *Nature* **2000**, *404*, 481. (c) Bernius, M. T.; Inbasekaran, M.; O'Brien, J.; Wu, W. *Adv. Mater.* **2000**, *12*, 1737.

(2) (a) Blom, P. W.; de Jong, M. J. M.; Vleggaar, J. J. M. *Appl. Phys. Lett.* **1996**, *68*, 3308. (b) Bozano, L.; Carter, S. A.; Scott, J. C.; Malliaras, G. G.; Brock, P. J. *Appl. Phys. Lett.* **1999**, *74*, 1132. (c) Crone, B. K.; Campbell, I. H.; Davids, P. S.; Smith, D. L. *Appl. Phys. Lett.* **1998**, *73*, 3162. (d) Martens, H. C. F.; Huiberts, J. N.; Blom, P. W. M. *Appl. Phys. Lett.* **2000**, *77*, 1852. (e) Pinner, D. J.; Friend, R. H. *J. Appl. Phys.* **1999**, *86*, 5116.

(3) Bernius, M.; Inbasekaran, M.; Woo, E.; Wu, W.; Wujkowski, L. *J. Mater. Sci.: Mater. Electron.* **2000**, *11*, 111.

(4) Chung, S.-J.; Kwon, K.-Y.; Lee, S.-W.; Jin, J.-I.; Lee, C. H.; Lee, C. E.; Park, Y. *Adv. Mater.* **1998**, *10*, 1112.

(5) (a) Chen, S.-A.; Lee, Y.-Z. *Poly(p-phenylenevinylene)s Modified with 2,5-Diphenylene-1,3,4-Oxadiazole Moieties as EL Materials*, Presented at the International Conference on Organic Electroluminescent Materials, September 14−17, 1996, Rochester, NY. (b) Lee, Y.-Z.; Chen, X.; Chen, S.-A.; Wei, P.-K.; Fann, W.-S. *J. Am. Chem. Soc.* **2001**, *123*, 2296. (c) Bao, Z.; Peng, Z.; Galvin, M. E.; Chandross, E. A. *Chem. Mater.* **1998**, *10*, 1201. (d) Jin, S.-H.; Kim, M.-Y.; Kim, J. Y.; Lee, K.; Gal, Y.-S. *J. Am. Chem. Soc.* **2004**, *126*, 2474. (e) Yu, L.-S.; Chen, S.-A. *Adv. Mater.* **2004**, *16*, 744.

(6) (a) Wu, F.-I.; Reddy, D. S.; Shu, C.-F. *Chem. Mater.* **2003**, *15*, 269. (b) Shu, C.-F.; Dodda, R.; Wu, F.-I.; Liu, M. S.; Jen, A. K.-Y. *Macromolecules* **2003**, *36*, 6698.

(7) Hung, M.-C.; Liao, J.-L.; Chen, S.-A.; Chen, S.-H.; Su, A.-C. *J. Am. Chem. Soc.* **2005**, *127*, 14576.

(8) (a) Chen, X.; Liao, J.-L.; Liang, Y.; Ahmed, M. O.; Tseng, H.-E.; Chen, S.-A. *J. Am. Chem. Soc.* **2003**, *125*, 636. (b) Granlund, T.; Pettersson, L. A. A.; Anderson, M. R.; Inganäs, O. *J. Appl. Phys.* **1997**, *81*, 8097. (c) Berggren, M.; Gustafsson, G.; Inganäs, O.; Andersson, M. R.; Hjertberg, T.; Wennerström, O. *J. Appl. Phys.* **1994**, *76*, 7530. (d) Lee, Y.-Z.; Chen, X.; Chen, M.-C.; Chen, S.-A. *Appl. Phys. Lett.* **2001**, 79, 308. (e) Turro, N. J. *Modern Molecular Phytochemistry*; Benjamin/Cummings Publishing Co.: Menlo Park, CA, 1978; pp 137−141.

(9) Chen, Y.-C.; Huang, G.-S.; Hsiao, C.-C.; Chen, S.-A. *J. Am. Chem. Soc.* **2006**, *128*, 8549.

(10) (a) Bliznyuk, V. N.; Carter, S. A.; Scott, J. C.; Klarner, G. G.; Miller, R. D.; Miller, D. C. *Macromolecules* **1999**, *32*, 361. (b) List, E. J. W.; Guentner, R.; Freitas, P. S.; Scherf, U. *Adv. Mater.* **2002**, *14*, 374.

(11) (a) Woudenbergh, T. V.; Wildeman, J.; Blom, P. W. M.; Bastiaansen, J. J. A. M.; Langeveld-Voss, M. W. *Adv. Funct. Mater.* **2004**, *14*, 677. (b) Chen, X.; Tseng, H.-E.; Liao, J.-L.; Chen, S.-A. *J. Phys. Chem. B* **2005**, *109*, 17496.

(12) (a) Graupner, W.; Leditzky, G.; Leising, G.; Scherf, U. *Phys. Rev. B* **1996**, *54*, 7610. (b) Meier, M.; Karg, S.; Zuleeg, K.; Brutting, W.; Schwoerer, M. *J. Appl. Phys.* **1998**, *84*, 87. (c) Tseng, H.-E.; Peng, K.-Y.; Chen, S.-A. *Appl. Phys. Lett.* **2003**, *82*, 4086. (d) Hong, C. M.; Day, D. E. *J. Appl. Phys.* **1979**, *50*, 5352.

(13) Evers, F.; Kobs, K.; Memming, R.; Terrell, D. R. *J. Am. Chem. Soc.* **1983**, *105*, 5988.

(14) Giro, G.; Cocchi, M.; Kalinowski, J.; Marco, P. D.; Fattori, V. *Chem. Phys. Lett.* **2000**, *318*, 137.

(15) (a) Klöpffer, W. *J. Chem. Phys.* **1969**, *50*, 2337. (b) Fujino, M.; Kanazawa, Y.; Mikawa, H.; Kusabayashi, S.; Yokoyama, M. *Solid State Commun.* **1984**, *49*, 575. (c) Yoshida, M.; Mitsui, S.; Kawai, T.; Kobayashi, N.; Hirohashi, R. *J. Polym. Sci., Part B: Polym. Phys.* **1999**, *37*, 61.

(16) Gallego, J.; Pérez-Foullerat, D.; Mendicuti, F.; Mattic, W. L. *J. Polym. Sci., Part B: Polym. Phys.* **2001**, *39*, 1272.